Inhibition of extracellular ice crystals growth for testing the cryodamaging effect of intracellular ice in a model of ram sperm ultra-rapid freezing

Filipp Georgijevic Savvulidi, Martin Ptacek, Anezka Malkova, Irena Kratochvilova, Daniel Simek, Felipe Martinez-Pastor & Ludek Stadnik

Published online: 02 Feb 2023.

Submit your article to this journal ↗

Article views: 884

View related articles ↗

View Crossmark data ↗

Citing articles: 1 View citing articles ↗

Taylor & Francis
Taylor & Francis Group

Inhibition of extracellular ice crystals growth for testing the cryodamaging effect of intracellular ice in a model of ram sperm ultra-rapid freezing

Filipp Georgijevic Savvulidi[a], Martin Ptacek [a], Anezka Malkova[a], Irena Kratochvilova[b], Daniel Simek[b], Felipe Martinez-Pastor[c] and Ludek Stadnik [a]

[a]Department of Animal Science, Faculty of Agrobiology, Food, and Natural Resources, Czech University of Life Sciences, Prague, Czech Republic; [b]Department of Functional Materials, Institute of Physics of the Czech Academy of Sciences, Prague, Czech Republic; [c]Instituto de Desarrollo Ganadero y Sanidad Animal (INDEGSAL) and Molecular Biology (Cell Biology), Universidad de Leon, Leon, Spain

ABSTRACT

We aimed to test the common belief, that as the sperm cell is the smallest cell in an organism and, therefore, it contains a small amount of intracellular water, the intracellular ice should not strongly affect the sperm cell during the cryopreservation. To investigate the effect of intracellular ice, we developed a novel approach of ram spermatozoa ultra-rapid freezing with the inhibition of the growth of extracellular ice crystals during freezing. In our approach, ram sperm was supplemented with cell-impermeable synthetic ice blocker 1,4-Cyclohexanediol, leaving a sample unsupplemented as a control. Sperm in cryostraws were ultra-rapidly frozen, and then thawed. We hypothesized, that only in the case when the intracellular ice plays the role in the cryodamage, the post-freezing intactness of spermatozoa frozen in the presence of extracellular ice inhibitors should be equal (or even less) to the intactness of spermatozoa frozen without extracellular inhibitors. No statistically significant difference ($p = 0.98$) was observed between the post-freezing intactness of sperm ultra-rapidly frozen in the presence of 1,4-Cyclohexanediol and the intactness of sperm frozen without 1,4-Cyclohexanediol. We concluded that the intracellular ice plays the role in sperm cryodamage, at least in the model of ram sperm ultra-rapid freezing.

Highlights

- Here, we investigated the cryodamaging factors during ram sperm ultra-rapid freezing;
- Optimized ultra-rapid freezing will provide positive economic implications for the sheep industry worldwide.

Introduction

Ultra-rapid freezing of livestock sperm is a very attractive technique of sperm freezing, which could eliminate some of the disadvantages of conventional sperm freezing (primarily, via the reduction of time of the freezing procedure and the elimination of the need of using expensive freezing equipment). Ultra-rapid freezing of sperm by its direct plunging into liquid nitrogen, in theory, should allow glass transition without the presence of ice crystals (due to the effect of vitrification). In practice, however, the achievability of the glass transition without the presence of ice crystals during the procedure of sperm ultra-rapid freezing is still questionable and great ambiguity in reports still exists. On the matter of extracellular environment, it was recently evidently shown, that the sperm ultra-rapid freezing technique failed to induce a glass-like state in the extracellular milieu and that the extracellular ice crystals with cell-damaging shapes (stretchmarks) were formed (Bóveda et al. 2020). On the matter of intracellular ice formation, some authors reported

no intracellular ice in the sperm heads after the ultra-rapid freezing (Morris 2006; Bóveda et al. 2020). These reports sound reasonable, as it is well known that the sperm heads have small cytoplasmic volumes, and the sperm cells contain very little intracellular water as the source of intracellular ice. Furthermore, some authors reported the possibility that only the absence of large, more damaging intracellular ice crystals can be observed by available laboratory techniques, without any possibility to observe the presence of small, yet damaging intracellular ice crystals (Bóveda et al. 2020). On the other hand, some authors did reveal evidence of sub-cellular distortion caused by the presence of lethal intracellular ice crystals in the peri-nuclear and peri-axonemal areas, possibly owing to a lack of sperm dehydration during the process of ultra-rapid freezing (Rodriguez-Martinez 2012). Because of such an ambiguity in the available reports, the possible role of intracellular ice crystals in the cryodamage of sperm during ultra-rapid freezing needs to be clarified further. This clarification might be a valuable tool for choosing an optimal strategy for improving the (generally low) results of livestock sperm ultra-rapid freezing procedure. This is especially so in the case of yet non-acceptable results of small ruminant sperm ultra-rapid freezing (Jiménez-Rabadán et al. 2015; Daramola and Adekunle 2016; Arando et al. 2017; Arando et al. 2019).

The biophysical behaviour of the cell in solution during freezing is known: during cell freezing, the extracellular space

is the primary place of the formation of ice crystals, which begins with the presence of nucleation sites (Honaramooz 2012). Because ice is pure crystalline water, during the crystal formation the extracellular space becomes highly hypertonic. This is due to the incorporation of water molecules in the growing ice crystals and the removal of salts from the ice crystals. Intracellular water moves outward across the plasma membrane due to the differential osmotic gradient and cell dehydration. The dehydration protects the cell from the retention of supercooled water within the cell and subsequent intracellular water crystallization (Fuller 2004). The approaches to block or inhibit the growth of extracellular ice crystals during cell freezing seem to be an interesting solution how to confirming the damaging effect of intracellular ice. Instead of trying to observe directly the intracellular ice during cell freezing (that is today still not a trivial task), the damaging effect of intracellular ice could be detected by the simple comparison of the intactness of spermatozoa frozen either with or without extracellular ice inhibitors. Importantly, such a comparison can be done with the use of well-developed laboratory techniques for sperm quality evaluation (such as flow cytometry). On this matter, we hypothesized that only in the case when the intracellular ice plays no role in the cryodamage (for example, because of small cytoplasmic volume, and by so because of no intracellular water inside the spermatozoa head during the freezing), the post-freezing intactness of spermatozoa frozen in the presence of extracellular ice inhibitors would be higher than the intactness of spermatozoa frozen without extracellular inhibitors (considering the absence of any cytotoxicity of used inhibitors). Oppositely, in the particular case when the intracellular ice plays the role in the cryodamage, the post-freezing intactness of spermatozoa frozen in the presence of extracellular ice inhibitors would be equal to or even less than the intactness of spermatozoa frozen without extracellular inhibitors. Our hypothesis is based on the simple mechanistic point of view: after the use of extracellular ice inhibitors and by so after the inhibition of the growth of extracellular ice crystals during cell freezing by ultra-rapid freezing, the cells would not lose their intracellular water fast enough, that would lead to spermatozoa cryodamage (mainly, on the level of their plasma membrane) due to formation of intracellular ice crystals (Figure 1). Therefore, the role of intracellular ice in cryodamage could be concluded from the abovementioned comparison.

In the present study, to inhibit the growth of extracellular ice crystals during the ultra-rapid freezing procedure confidently, the high concentration of cell-impermeable synthetic ice blocker 1,4-Cyclohexanediol (1,4-CHD) was used. Previously, its cryoprotective potential has been demonstrated in the procedure of slow freezing of ram spermatozoa; it was hypothesized that its cryoprotective ability is due to the inhibition of ice crystal growth, albeit with no direct physical confirmation (Quan et al. 2013; Quan et al. 2015).

To the best of our knowledge, however, there have been no previous studies utilizing the inhibitory effect of 1,4-CHD synthetic ice blocker upon extracellular ice crystal growth to investigate the role of intracellular ice crystals in the cryodamage of sperm during the procedure of ultra-rapid freezing. The general aims of the present study were, therefore: 1)

confirm physically the ability of 1,4-CHD to inhibit the growth of extracellular ice crystals in the freezing medium of choice with the use of X-ray diffraction analysis (XRD); 2) confirm the nontoxic nature of 1,4-CHD upon sperm cells; 3) with the use of flow cytometry, compare of the intactness of spermatozoa frozen without, or with 1,4-CHD extracellular ice inhibitor, and by so investigate the role of intracellular ice in the cryodamage of ram sperm cells during the procedure of ultra-rapid freezing, accordingly to our hypothesis; 4) with the use of scanning electron microscopy, compare the plasma membrane structure of spermatozoa frozen without, or with 1,4-CHD extracellular ice inhibitor to observe the destruction of spermatozoa plasma membrane induced by intracellular ice.

Materials and methods

Methodology used to fulfil the first aim

X-ray diffraction analysis and statistics

The spermatozoa-free samples of glycerolated AndroMed commercial egg yolk-free semen extender (Minitüb GmbH, Tiefenbach, Germany) were supplemented either with no 1,4-CHD or with 300 mM of 1,4-CHD (final concentration; Sigma Aldrich, St. Louis, Missouri, USA) was prepared. The 1,4-CHD stock solution was prepared by dissolving 1,4-CHD in Dulbecco's phosphate-buffered saline without divalent cations (Biosera Europe, Nuaille, France). The sample without 1,4-CHD consisted solely of spermatozoa-free AndroMed and the same volume of spermatozoa-free Dulbecco's phosphate-buffered saline as in the sample supplemented with 1,4-CHD. XRD was performed according to the procedure established at the Department of Functional Materials, Institute of Physics of the Czech Academy of Sciences, Prague, Czech Republic. Briefly, samples were placed in an aluminum cuvette and covered with 10 micron Mylar foil. Afterward, they were cooled in an in-situ X-ray low-temperature chamber (Anton Paar DCS 350, Anton Paar GmbH, Graz, Austria) with a maximum cooling rate of 0.1 K per second down to −30 degrees centigrade and measured at −30, −20, −10, −6, −4 and −2 degrees consequently or until meltdown. The last temperature was a reference measurement of a molted sample. Each measurement was performed using a Bruker D8 diffractometer (Bruker, Billerica, Massachusetts, USA) equipped with a copper rotating anode generator (40 kV, 300 mA) and parabolic Goebel mirror producing a parallel primary beam (horizontally) with a 4-degree vertical divergence limited by Soller slits. The diffracted intensity was acquired using a constant slit detector set at a constant 2theta angle of 39.85 degrees. The sample under non-ambient conditions was inclined with the incident angle between 5 and 35 degrees in steps of 0.02 degrees and tilted around the horizontal axis from −4 to +16 degrees by steps of 2 degrees. The steps were approximately one-half of the efficient angular resolution in both cross-sectional directions. Recorded intensities were statistically analyzed. The background angular dependence was estimated from the smoothed measurement of the completely melted sample at the highest temperature; the precise background
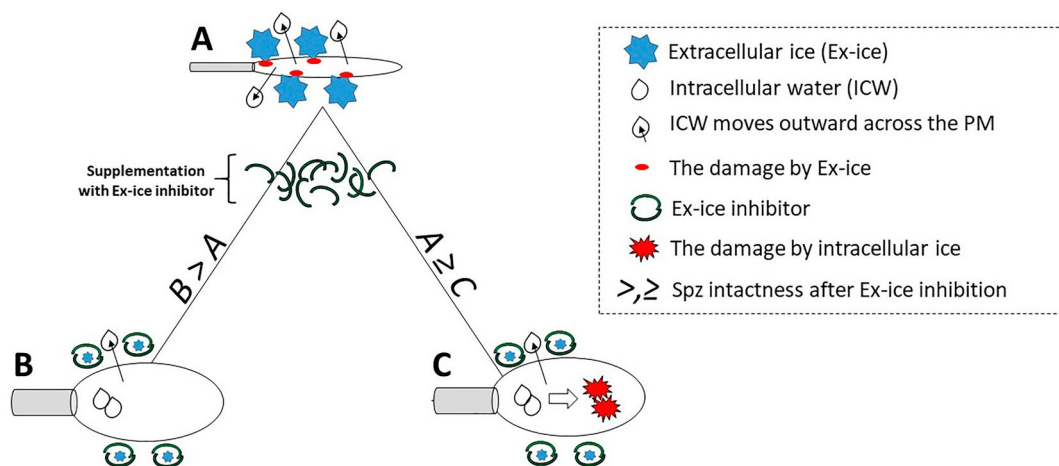
Figure 1. Indirect evaluation of the role of intracellular ice in the sperm cryodamage, a hypothesis. From a mechanistic point of view, three possible scenarios could take a place after spermatozoa ultra-rapid freezing either without (A), or with extracellular ice inhibitor supplementation (B, C). In scenario A, growing extracellular ice reduce effectively the amount of intracellular water and cells are dehydrating. However, the sperm plasma membrane might be compromised after the impact of growing extracellular ice. In scenario B, the damaging impact of extracellular ice will be suppressed by the use of an extracellular ice inhibitor. As the damaging impact of extracellular ice is suppressed, and as there are no other damaging impacts considered, the post-freezing intactness of cells in B should be higher than in A (B > A). In scenario C, again the damaging impact of extracellular ice will be suppressed by the use of extracellular ice inhibitors. However, at the same time, the process of cell dehydration will be suppressed too. The cell will retain intracellular water and damaging crystals of intracellular ice will be formed during ultra-rapid freezing. Therefore, the post-freezing intactness of cells in C will be lower (or equal) than in A (C ≤ A).

level factor for each temperature (due to varying amorphous parts of the sample) was determined by a statistical law of Poison noise so that the average squared negative difference of measured photon counts from the background level would contribute by one half to the expected value equal to a number of photon counts of expected background. The Poison statistic assumes that $\langle (N_i - \langle N_i \rangle)^2 \rangle = \langle N_i \rangle$, where N_i is a number of expected background photon counts for a particular inclination angle defined as a constant multiple of photon counts for the same angle measured with a completely melted sample ($N_i = k*N_{ibgnd}$); the constant (k) is varied to fulfil the above-mentioned condition. Intensities exceeding the noise level above the background are then considered statistically relevant for further processing. The processing of the data by the deconvolution procedure was described in Kratochvílová et al. (2017), and the result is the distribution histogram of the volume portion of diffracting crystallites in the specimen dependent on their diffracting volume. The method does not allow for quantitative calibration of the volume scale (the crystal sizes are in the order of microns), but it allows for comparison between particular temperatures and the tendencies can be compared between several similar samples.

Methodology used to fulfil the second and third aims

Animals and semen collection

Except for semen collection by artificial vagina, the present study did not involve any animal in vivo experiments. Therefore, the review board of the Expert commission ensuring the welfare of experimental animals at the Czech University of Life Sciences in Prague considers that this type of project does not fall under the legislation for the protection of animals used for scientific purposes (Act no. 246/1992 Sb.). It considers that this type of research has no impact on animal welfare because only non-experimental agricultural practices (in accordance with Act no. 166/1999 Sb. and Act no. 154/2000 Sb.) were used during the study.

The procedures of electro-ejaculator semen collection were performed in accordance with the Instituto de Desarrollo Ganadero y Sanidad Animal institutional standards for the care and welfare of animals, which conforms to the European Union Directive 86/609 regarding the protection of animals used in scientific experiments.

Animal management and semen collection procedure were previously described (Savvulidi et al. 2021). If not indicated otherwise, two mature original Wallachian rams from the Genetic Resources of the Czech Republic were used in the present study. Wallachian rams with typical exterior signs of the breed and with an excellent breeding history were transported from the area of the Beskids Mountains. Afterward, animals were kept at the Demonstration and Experimental Centre of the Czech University of Life Sciences in Prague (GPS coordinates: 50°07′47.6″N 14°22′07.0″E), at the nearest distance to the laboratory of flow cytometry. This was done with a special intention to reduce any variability due to possible delays between the collection of semen and its subsequent evaluation. Also, this enabled to use of rams in the same health condition under strict veterinary inspection, in the same breeding conditions, under the same feeding ration, with the semen collected and processed in the same manner and in the same time duration. Semen was naturally collected using a sheep/goat artificial vagina (AV) (Minitüb GmbH, Tiefenbach, Germany) prepared according to the manufacturer's instruction manual. Semen was collected in November – December 2019 and January – February 2020 periods; at the end of a natural mating season (which is from the beginning of August to the beginning of December for the breeding conditions of the Czech Republic). On the day of semen collection (n = 8 collection days, in total), the semen of the 1st ejaculate

was collected from each ram individually. Samples were collected twice a week at most, with a minimum of 1-day pause between any two adjacent semen collections.

Semen processing and 1,4-CHD supplementation

Immediately after collection (except in the samples intended for mass motility evaluation), collected semen was extended 1:4 (v/v) with the glycerolated AndroMed commercial egg yolk-free semen extender (Minitüb GmbH, Tiefenbach, Germany) prepared according to the manufacturer's instruction manual. The exact concentrations of glycerol and lecithin in this commercial extender are proprietary; according to available literature, it contains around 7% of glycerol (Akçay et al. 2012) and 1% of soya lecithin (Miguel-Jimenez et al. 2020). Extended semen was delivered to the laboratory within 1 h, at ambient transport temperature.

The mass motility was evaluated subjectively in undiluted semen, using a 0 (no mass motility) up to 5 (greatest mass motility) scores scale according to David et al. (2015). Only semen of good initial quality (scored 3, or higher) was used for further processing.

Spermatozoa concentration in extended Wallachian sperm was evaluated using a pre-calibrated spectrophotometer (Genesys 10S Vis, Thermo Fisher Scientific, Waltham, Massachusetts, USA). The extended semen was then diluted to a final concentration of 40 million/mL with an AndroMed extender.

After the final dilution, sperm samples were supplemented with 1,4-CHD, leaving a sample unsupplemented as a control. The 1,4-CHD stock solution was prepared by dissolving 1,4-CHD in Dulbecco's phosphate-buffered saline without divalent cations. Sperm were divided into two groups for 1,4-CHD supplementation: 0, and 300 mM (final concentration). The control received only Dulbecco's (same volume as in other groups). The osmolality of the treatments was checked with an Osmomat 3000 M, a single-sample freezing point osmometer (Gonotec GmbH, Berlin, Germany). The measured osmolality (mOsmol/kg ± S.D.) was: 1486.0 ± 12.7 for 0 mM and 2137 ± 9.89 for 300 mM.

Sperm cooling and equilibration

0.25 mL French straws (IMV Technologies, L'Aigle, France) were loaded with sperm and sealed with polyvinyl alcohol (PVA) powder. Sealed straws were transferred to the refrigerator for cooling (cooling rate 1.0 °C per min, on average) and subsequent equilibration at 4–6 °C for 2–4 h (Lv et al. 2019).

Ultra-rapid freezing procedure and sperm thawing

Sperm in straws was ultra-rapidly frozen by its immediate one-by-one vertical immersion into liquid nitrogen with simultaneous rotation of the straws (to prevent straw burst). Straws were stored in liquid nitrogen for at least 24 h before thawing. Samples were thawed in a water bath, at 37 °C for 30 s (Jiménez-Rabadán et al. 2015).

Slow freezing and sperm thawing

In the present study, to evaluate the general freezability of the collected Wallachian sperm, slow sperm freezing was used as an alternative to ultra-rapid freezing. Semen was collected and processed before freezing as described in section 'Animals and semen collection'. For slow freezing, straws were frozen in the egg yolk-free freezing extender AndroMed by their static exposure to liquid nitrogen vapour for 10 min 4 cm above the LN_2 surface, a common freezing technique widely applied for livestock sperm cryopreservation (Barbas and Mascarenhas 2009). Samples were thawed in a water bath, at 37 °C for 30 s.

Flow cytometric evaluation of sperm parameters before equilibration, after equilibration, and immediately after thawing

We used a flow cytometric panel (named Panel 1) for the evaluation of intact spermatozoa before/after equilibration and immediately after thawing. Intact spermatozoa were defined as the proportion of spermatozoa sharing some desirable characteristics (intact plasma membrane, intact acrosome, high mitochondrial potential). To determine the effect of freezing, intact spermatozoa were analyzed pre-freezing (after the equilibration), and post-thawing. The percentage of preserved intact spermatozoa (x) in thawed sperm was calculated using the formula: x = (intact spermatozoa in thawed sperm* 100) / (intact spermatozoa in equilibrated sperm). Excel's two-tailed T.TEST (two samples equal variance) function was used in the present study for statistical analyses of flow cytometric data. Statistical analyses were calculated with a significance level set at a 5% cutoff ($p < 0.05$).

For Panel 1, the Wallachian sperm samples were added to 250 µl of Dulbecco's at 4 million/mL and stained for 10 min at 38 °C in the dark with the following probes (final concentration given): 16.2 µM Hoechst-33342 (H-342) for discriminating debris; 12 µM propidium iodide (PI) for assessing plasma membrane damage; 0.5 µg/mL PNA-FITC for assessing the acrosomal status; and 80 nM Mitotracker Deep Red (MTR DR) for assessing mitochondrial activity. Fluorochromes H-342 and PI were purchased from Sigma Aldrich (St. Louis, Missouri, USA), and PNA-FITC and MTR DR were obtained from Thermo Fisher Scientific (Waltham, Massachusetts, USA). Subsequently, sperm samples were analyzed using a NovoCyte digital flow cytometer, model 3000 (Acea Biosciences, part of Agilent, Santa Clara, California, USA). The flow cytometer was equipped with violet (405 nm), blue (488 nm), and red (640 nm) lasers and appropriate optical filters for the detection of emitted fluorescence signals. The fluorescence was collected using optical filters 445/45 (violet laser, H-342), 530/40 (blue laser, PNA-FITC), and 675/30 (blue line, red fluorescence: PI), and 675/30 (red line, red fluorescence: MTR DR). The samples were run at low speed (14 µl/min) and at least 10000 total events were recorded for each sample. NovoExpress software, version 1.3.0 (Acea Biosciences, part of Agilent, Santa Clara, California, USA) was used for automated cytometer setup and performance tracking as well as data acquisition. The same software was also used to analyze acquired flow cytometry data. No compensation was required with the optical filter setup used.

To investigate the effect of prolonged exposure of chilled ram sperm to 1,4-CHD, semen from two Assaf adult healthy rams belonged to the flock at a private sheep breeding farm located in the Castilla y León autonomous community, Spain (GPS coordinates: 42°33′41.2″N 5°52′36.1″W) was used. Assaf semen was collected with the use of electro ejaculator

Minitüb® e320 (Minitüb GmbH, Tiefenbach, Germany), as a part of a survey programme promoted by the breeders' association. Semen was collected during October 2019. On the day of semen collection (n = 3 collection days, in total), semen was collected and immediately extended 1:4 (v/v) with the glycerol-supplemented AndroMed commercial egg yolk-free semen extender. A time interval of a minimum of 2 days was applied between any two adjacent semen collections. CASA (Computer Assisted Sperm Analysis) was used to analyze the initial motility and concentration of spermatozoa in Assaf sperm. It consisted of an E400 Nikon microscope (Nikon Corp, Tokyo, Japan) with a 10X phase contrast and 37℃ stages, Basler A312fs digital camera (Basler AG, Ahrensburg, Germany), a Makler counting chamber, 10 µm deep (Sefi-Medical Instruments, Haifa, Israel) and the ISAS software (Proiser, Paterna, Spain). All sperm samples collected from Assaf rams demonstrated adequate initial motility characteristics (>70% total motility). The extended semen was diluted to a final concentration of 40 million/mL with an AndroMed extender. After the final dilution, sperm was supplemented with 300 mM (final concentration) of 1,4-CHD, leaving a sample unsupplemented as a control (0 mM). Sperm samples were filled into 0.25 mL French straws and sealed with PVA powder. Sealed straws were transferred to the refrigerator for cooling and subsequent equilibration at 4 - 6 ℃ for 12 h (extended time of equilibration). After equilibration, two flow cytometric panel (named Panel 2) was used for the evaluation of intact spermatozoa. For Panel 2, flow cytometry analyses were conducted according to the standard protocol established at INDEGSAL. Briefly, the CyAn ADP (Beckman Coulter; Brea, CA, USA) flow cytometer equipped with three diode lasers (violet – 405 nm, blue – 488 nm, and red – 635 nm) was used. Assaf sperm samples were added to 300 µl of PBS with 0.5% bovine serum albumin at 10 million/mL and stained with fluorescent probes (ThermoFisher; Waltham, MA, USA) for 15 min at 37 ℃, with final concentrations as follows: 4.5 µM H-342 for discriminating debris; 100 nM YO-PRO-1 for assessing apoptosis-associated changes; 2 µM merocyanine 540 (M-540) for assessing capacitation-associated changes; 1.5 µM PI for assessing plasma membrane damage; 100 nM MTR DR for assessing mitochondrial activity via mitochondrial membrane potential. At least 5000 spermatozoa were collected per sample, with a flow rate of 200 cells/s. Acquired flow cytometry data were analyzed using the NovoExpress software, version 1.3.0 (Acea Biosciences, part of Agilent, Santa Clara, California, USA). Statistical analyses were calculated using Excel's two-tailed T.TEST (two samples equal variance) function with a significance level set at a 5% cutoff ($p < 0.05$).

Methodology used to fulfil the fourth aim

Scanning electron microscopy

In the present study, scanning electron microscopy (SEM) was used to observe the evidence of sub-cellular distortion on ram spermatozoa, potentially caused by the presence of intracellular ice crystals during the process of ultra-rapid freezing. For this, the semen from two adult healthy Suffolk rams belonged to the flock at a private sheep breeding farm located in the Central Bohemian Region, Czech Republic (GPS coordinates: 49°55′27.8″N 14°49′59.2″E) was used. Semen from Suffolk rams

was naturally collected using a sheep/goat artificial vagina (AV) prepared according to the manufacturer's instruction manual. Semen was collected in April 2019. On the day of semen collection (n = 1 collection day), the semen of the 1st ejaculate was collected from each ram individually. Immediately after collection (except in the samples intended for mass motility evaluation), semen was extended 1:4 (v/v) with the glycerol-supplemented AndroMed commercial egg yolk-free semen extender. The mass motility was evaluated as described above. Only semen of good initial quality (scored 3, or higher) was used for further processing. Spermatozoa concentration in extended Suffolk sperm was subjectively evaluated with the Bürker counting chamber under a basic light microscope. The extended semen was then diluted to a final concentration of 40 million/mL with an AndroMed extender. After the final dilution, sperm was divided into two groups during 1,4-CHD supplementation: 0 mM (control) and 300 mM (final concentration). Sperm samples were filled into 0.25 mL French straws and sealed with PVP powder. Sealed straws were transferred to the refrigerator for cooling and subsequent equilibration at 4 - 6 ℃ for 2–4 h. Sperm in cryostraw were vitrified by its immediate vertical immersion into liquid nitrogen with simultaneous rotation of the straw. Vitrified straws were stored in liquid nitrogen for at least 24 h before thawing. Thawed sperm samples were processed according to the standard SEM protocol established at the Laboratory of Electron Microscopy, Faculty of Science, Charles University in Prague, Czech Republic. Briefly, pellets of spermatozoa were fixed for 24 h in 2.5% glutaraldehyde in 0,1 M cacodylate buffer (pH 7.2) and postfixed in 2% OsO_4 in the same buffer. Fixed samples were dehydrated through an ascending concentration series of ethanol (the last step was acetone) and dried by Bal-Tec CPD 030 CO2 critical point dryer (BAL-TEC AG, Balzers, Liechtenstein). Samples were coated with gold (2 nm thin layer) in a Bal-Tec SCD 050 ion sputter coater (BAL-TEC AG, Balzers, Liechtenstein) and observed with a JEOL 6380 LV microscope (JEOL Ltd. Tokyo, Japan) under accelerating voltage of 25 kV.

Results

Results on the first aim

1,4-CHD Strongly inhibits extracellular ice crystal growth in spermatozoa-free semen extender during freezing

To fulfil the first aim, we confirmed physically the ability of 1,4-CHD to inhibit the growth of extracellular ice crystals in the AndroMed freezing medium with the use of X-ray diffraction analysis. The frozen solution crystals distribution was measured and compared for basic solution and solution containing 300 mM 1,4-CHD. The recorded XRD data are represented in an intensity map in χ (vertical) and ω (horizontal) angles representing about 1/17 of all possible crystal space orientations, for specimens without (Figure 2a) and with 300 mM 1,4-CHD (Figure 2b). Each ice crystal generates a peak of about the same vertical and horizontal span, which is defined by the resolution of the diffractometer. The peak intensity of each spot is proportional to the volume of the crystallite attenuated by the absorption of the water (ice) above the diffracting crystal that is not in a diffracting condition. Thus, uniform-sized crystals
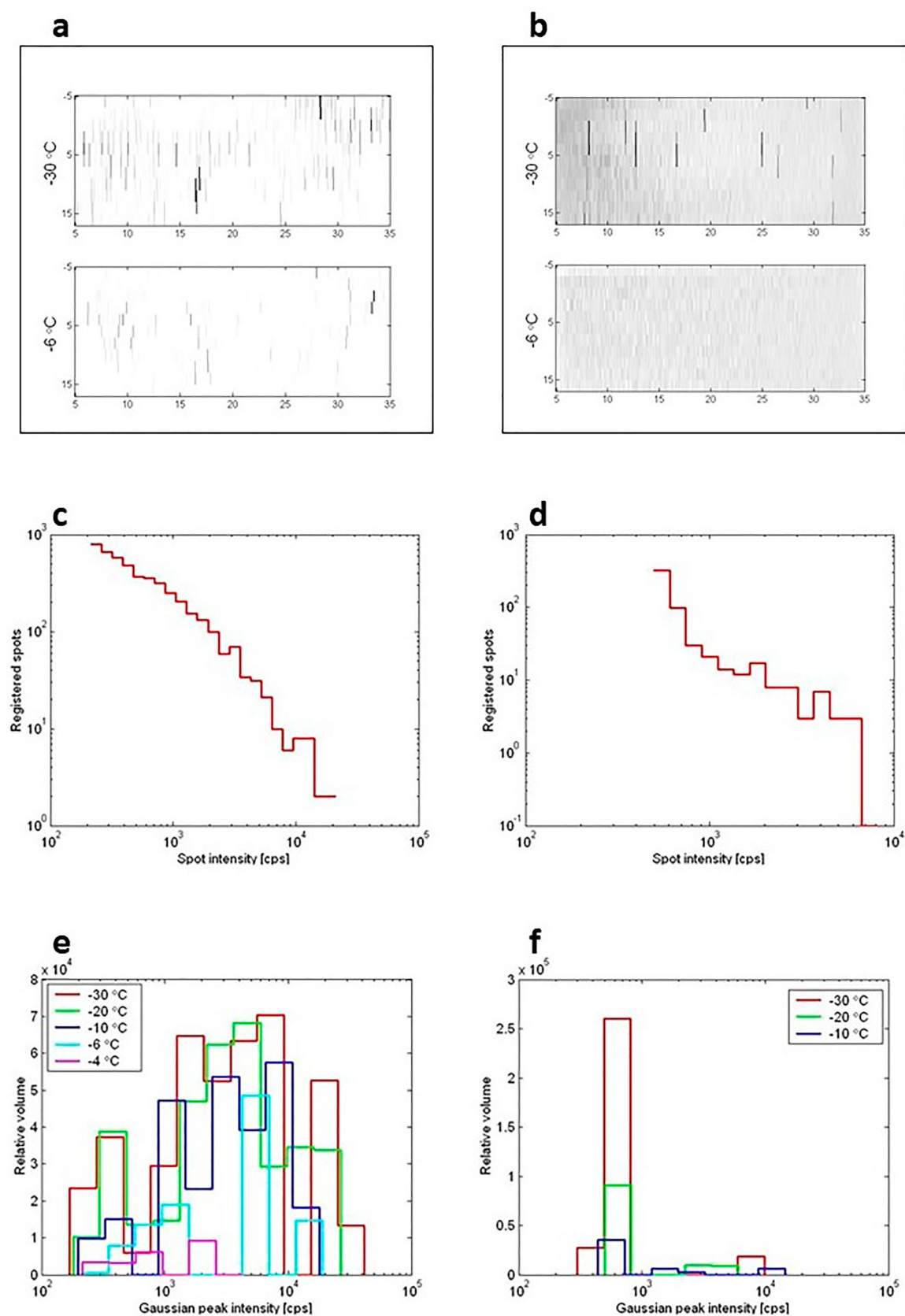
Figure 2. Results of X-ray diffraction analysis. a,b Measured angular dependence of diffracted intensity of 110 ice diffraction peak for specimens without (a) and with 300 mM 1,4-CHD (b). The logarithmical grey scale is different for the specimens as indicated by the noise level background visible in (b) and suppressed by larger scaling in (a). The strongest peaks are 2x oversaturated to enhance the visibility. Each peak represents diffraction from one ice crystal. The resolution in vertical axis is ten times worse (hence the anisotropy of the spots). At −30°C both specimens are fully frozen, at −6°C the crystallites in specimen without 1,4-CHD (a) are partially molten, while the specimen with 1,4-CHD (b) is fully molten (only noise is visible). c,d Area intensity distribution histograms. Recorded statistics of a number of measurement points (vertical axis) at −30°C with diffracted intensity in certain logarithmically spaced ranges (horizontal axis) for specimens without (c), and with 300 mM 1,4-CHD (d). The horizontal scale of the histogram is cut off at the noise level from the left and the maximum observed intensity from the right. e,f Diffraction volume distribution histograms. XRD analysis of two samples of AndroMed supplemented with or without 1,4-CHD. The range (horizontal axis) scales start at intensity levels that are safely over the noise level – it corresponds to the size of crystallites. The vertical scale is either the number of data points with the specified intensity – the number of crystallites of a specified size. e frozen/molten pure solution-0 mM 1,4-CHD; f frozen/molten solution containing 300 mM 1,4-CHD. cps – counts per second.

would produce a distribution of peaks from maximum intensity down to zero with an exponential drop in probability. Each peak, as well, has exponentially dropping tails.

The total intensity statistics for specimens without (Figure 2c) and with 300 mM 1,4-CHD (Figure 2d) thus would exhibit a typical statistical profile for each crystal volume present in the specimen. The shape is similar to Figure 2d between 10^3 and 10^4 cps of diffracted intensity.

The increase around 4×10^2 cps comes from the smaller crystallites that represent the highest peak in Figure 2f. The crystal volume distribution is deconvoluted from the intensity statistics and renormalized to the volume that particular crystal sizes represented in the sample (10 small crystals represent the same volume as one 10 times larger crystal).

Figure 2e,f shows histograms counting the data points whose diffraction intensities lay in the particular ranges for each of the plots from X-ray diffraction measurements performed on samples at different temperatures. The horizontal axis scales start at intensity levels that are safely over the noise level – it corresponds to the size of crystallites. The vertical scale is the number of data points with the specified intensity – which corresponds to the number of crystallites of a specified size. According to the kinematical theory of XRD, the diffraction intensity of crystallites (x-axis in Figure 2e,f) is proportional to their volume. The histograms in Figure 2e,f count the relative sample volume occupied by crystals with particular ranges of diffraction magnitude (proportional to crystal volume). The linear dimension (diameter) of the ice crystals is roughly the third root of the diffracting volume. The reference of the pure sample (without 1,4-CHD) shows a broad statistical distribution of ice crystallites after freezing (Figure 2e) ranging over more than two orders in volume (i.e. about 5 times in diameter) – red curve for crystallites at −30 °C. The distribution does not change significantly with raising temperature but for its overall decrease. This indicates that the crystals melt randomly regardless of their original size. At −2 °C, the sample is completely melted.

In a sample supplemented with 300 mM 1,4-CHD (Figure 2f), the growth of crystals appears to be inhibited to a large extent. The melting procedure of frozen 300 mM 1,4-CHD solution is again random, for there is no horizontal shift in crystal volume distribution – only an obvious statistical occurrence default. At −6 °C, the sample was completely molten.

We did not observe gradual downsizing or crystal growth (recrystallization) in any of our samples, therefore we conclude that neither composition-gradient ice crystals were formed during the freezing process, nor the crystal size was limited by the freezing rate (and limited diffusion rate), but rather the crystal sizes on freezing were determined by the concentration of 1,4-CHD in the water. Crystal size remained constant until the solution around a particular crystal triggered its melting.

Results on the second aim

1,4-CHD Supplementation has no cytotoxic impact on equilibrated spermatozoa

To fulfil the second aim of the present study, we confirmed the nontoxic nature of 1,4-CHD in sperm cells. In the present study, a statistically significant damaging effect of equilibration on sperm quality was observed. This effect was manifested regardless of the supplementation of 1,4-CHD, and already on the level of plasma membrane damage ($25.4 \pm 3.97\%$ of PI-positive events before equilibration versus $37.2 \pm 7.25\%$ of PI-positive after equilibration, $p > 0.05$). As the quality of sperm plasma membrane is an integral part of the complex variable 'intact spermatozoa', observed a decrease in the quality of plasma membrane can explain a relatively low percentage of intact spermatozoa in post-equilibrated sperm observed in our study with the use of Panel 1 (Figure 3a). Nevertheless, Figure 3a shows a lack of any cytotoxic impact of 1,4-CHD supplementation during the sperm equilibration on the intact spermatozoa. Importantly, even after the extended time (12 h) of equilibration of ram sperm supplemented with 1,4-CHD, there was no observable decrease in the intact spermatozoa due to the 1,4-CHD supplementation post-equilibration (Figure 3b).

Results on the third aim

Inhibition of extracellular ice by 1,4-CHD does not improve the results of ram sperm ultra-rapid freezing

To fulfil the third aim, we with the use of flow cytometry, compared the intactness of spermatozoa ultra-rapidly frozen without, or with 1,4-CHD extracellular ice inhibitor. Preserved intact spermatozoa obtained in ultra-rapid freezing sperm with AndroMed was very low immediately after thawing (preserved intact spermatozoa was below 1%), regardless of 1,4-CHD supplementation. No statistically significant impact of 1,4-CHD on the preserved intact spermatozoa after ultra-rapid freezing was observed (Figure 3c).

The plasma membrane was identified as the place of the primary site of damage in ultra-rapidly frozen spermatozoa by its excessive (> 99%) PI-positivity observed by flow cytometry. Importantly, in our study, the preserved intact spermatozoa were as high as $18.0 \pm 7.57\%$ (mean ± SD) if sperm samples were slowly frozen (Figure 3d).

Results on the fourth aim

Supplementation with 1,4-CHD leads to severe damage of the plasma membrane in ultra-rapidly frozen spermatozoa

To fulfil the fourth aim, we with the use of scanning electron microscopy, compare the plasma membrane structure of spermatozoa ultra-rapidly frozen without, or with 1,4-CHD extracellular ice inhibitor. Severe plasma membrane damage (membrane openings, Figure 4d; arrows) was observed by SEM in ultra-rapidly frozen ram spermatozoa supplemented with 1,4-CHD. Less evident plasma membrane damage was observed on ultra-rapidly frozen spermatozoa without 1,4-CHD supplementation (Figure 4c; arrows). In our study, no plasma membrane damage was observed in non-frozen sperm after its equilibration with or without the presence of 300 mM 1,4-CHD (Figure 4a,b).

Discussion

In our study, we aimed to test the common belief, that as the sperm cell is the smallest in an organism and, therefore, it contains a relatively small amount of intracellular water, the
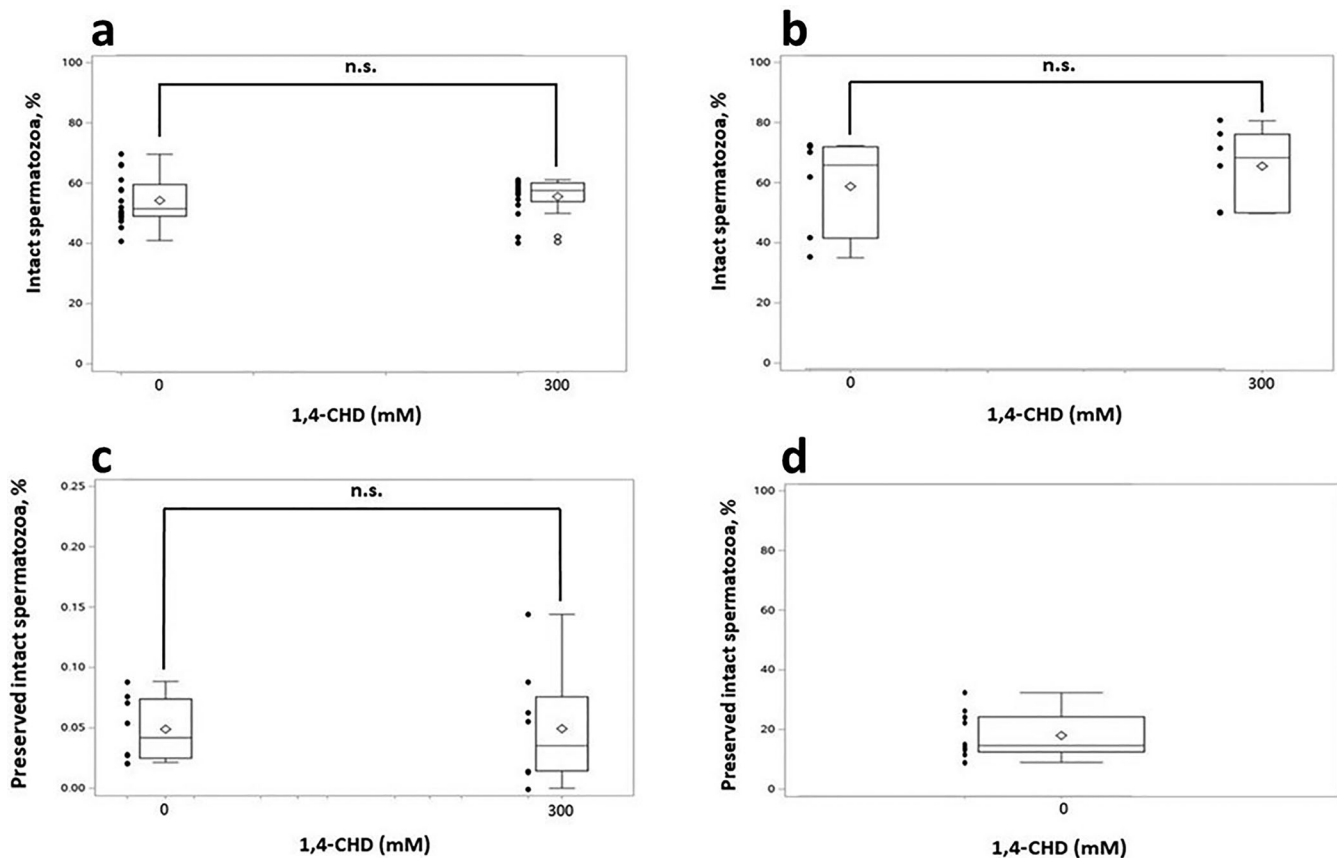
Figure 3. Results of flow cytometry. a Box-and-whisker plots of intact spermatozoa (%) in equilibrated ram sperm as evaluated by flow cytometry. Wallachian sperm equilibrated for 2–4 h. Each bar represents the measurement result from eight collection days (two technical replicates per day). To exclude any ram-to-ram variability, pooled data for rams are presented. The diamond symbol indicates the mean value. n.s. indicates no statistically significant difference ($p = 0.6$). b Box-and-whisker plots of the intact spermatozoa (%) after a prolonged time of equilibration as evaluated by flow cytometry. Assaf sperm was equilibrated for 12 h and then was analyzed with FC panel 2 (H342+/YO-PRO-1-/M-540-/PI-/MTR DR+). Each bar represents the measurement result of intact spermatozoa from three different collection days (two technical replicates per day). To exclude any ram-to-ram variability, pooled data for rams are presented. The diamond symbol indicates the mean value. n.s. indicates no statistically significant difference ($p = 0.5$). c Box-and-whisker plots of preserved intact spermatozoa (%) in ultra-rapidly frozen Wallachian sperm. Preserved intact spermatozoa immediately after thawing, as evaluated by Panel 1. Each bar represents the measurement result from four different collection days (two technical replicates per day). To exclude any ram-to-ram variability, pooled data are presented. The diamond symbol indicates the mean value. n.s. indicates no statistically significant difference ($p = 0.98$). d Box-and-whisker plot of preserved intact spermatozoa (%) in slowly frozen Wallachian sperm. The percentage of the preserved intact spermatozoa immediately after thawing, as evaluated by Panel 1 is presented. The plot represents the result of preserved intact spermatozoa in group control (0 mM) from six different collection days (two technical replicates per day). To exclude any ram-to-ram variability, pooled data are presented. The diamond symbol indicates the mean value.

intracellular ice should not strongly affect the sperm cell state during the cryopreservation. This is opposite to the cryopreservation of oocytes (containing a large amount of intracellular water), where the cryodamaging effect of intracellular ice is great (Tsuzuki et al. 2000). Indeed, some authors reported no intracellular ice in the sperm heads after the ultra-rapid freezing (Morris 2006; Bóveda et al. 2020). On the other hand, some authors reported the possibility that only the absence of large, more damaging intracellular ice crystals can be reliably observed, without any possibility to observe the presence of small, yet strongly damaging intracellular ice crystals (Bóveda et al. 2020). Moreover, some authors did reveal evidence of sub-cellular distortion caused by the presence of lethal intracellular ice crystals during the process of ultra-rapid freezing (Rodriguez-Martinez 2012). Generally speaking, the results of the work of many authors support the idea about damage to the sperm membrane upon cryopreservation due to the formation of intracellular ice, which corrupted the spermatozoon plasma membrane by changing its organization, fluidity, permeability, or lipid composition (Xin et al. 2019). Because there

is no unambiguous point of view exists on the role of intracellular ice in the cryodamage of sperm cells during sperm cryopreservation by ultra-rapid freezing technique, no optimal strategy of how to improve the low results of (livestock) sperm ultra-rapid freezing procedure can exist either. Therefore, it is important to investigate the role of intracellular ice in cryodamage to find an optimal strategy to improve the results of ultra-rapid freezing. Interestingly, human sperm cells can survive ultra-rapid freezing and thaw relatively easily even without the application of permeable cryoprotectants (Isachenko et al. 2012). However, a very small volume of sperm is usually used for the ultra-rapid freezing procedure of human sperm to achieve a high cooling rate. Ultra-rapidly frozen human sperm can only be further used in the procedure of assisted reproduction (such as intracytoplasmic sperm injection). In livestock, the sperm must be ultra-rapidly frozen in much larger volumes to make practical the artificial insemination with frozen sperm doses (250 microliters, at least; preferably frozen inside standard cryostraws, not in the microdroplets). The above-mentioned fact introduces evident obstacles
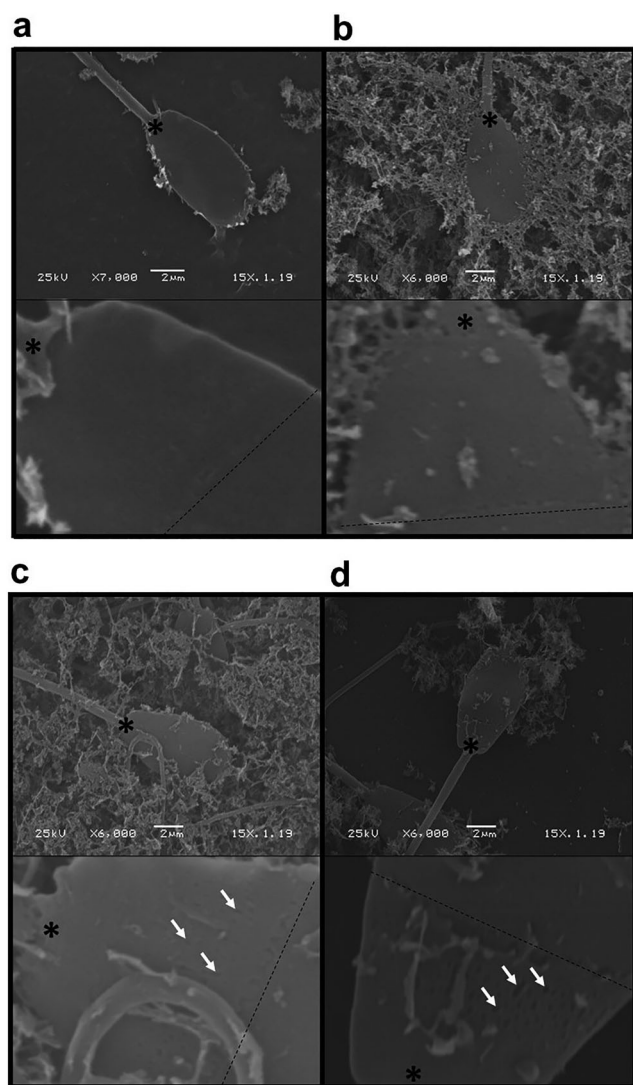
Figure 4. Scanning electron microscopy of spermatozoa. a Equilibrated, non-frozen sperm without 1,4-CHD supplementation; b Equilibrated, non-frozen sperm supplemented with 300 mM 1,4-CHD; c ultra-rapidly frozen sperm without 1,4-CHD supplementation; d ultra-rapidly frozen sperm supplemented with 300 mM 1,4-CHD. The dashed line represents the position of the post-nuclear sheath border; the asterisk marks the position of the posterior ring. Illustrative scans (top panel) and corresponding crops (lower panel) are shown.

which make livestock sperm ultra-rapid freezing procedure much less successful in comparison to human sperm ultra-rapid freezing.

In our study, we used commercially available egg yolk-free glycerolated AndroMed semen extender as a freezing medium. According to the manufacturer, the AndroMed semen extender was developed for conventional slow freezing of bull sperm with the use of automatic semen freezers, or the preservation of fresh semen, but not for sperm ultra-rapid freezing. This might cause doubts about its usage in the procedure of ram sperm ultra-rapid freezing. On the other hand, AndroMed is an egg yolk-free, soybean lecithin-based extender. Nowadays, despite numerous reported mechanisms of egg yolk-related cryoprotection, and despite the beneficial effects of egg yolk in the procedures of ram sperm slow freezing (Ptáček et al. 2019), there is a movement worldwide to omit, or substitute egg yolk in livestock semen extenders, as it might

seriously diminish the quality of frozen-thawed spermatozoa (Bousseau et al. 1998; Aires et al. 2003; Shu Shan et al. 2009; Najafi et al. 2014; Miguel-Jimenez et al. 2020; Zakošek Pipan et al. 2020). Soybean lecithin, as an alternative to egg yolk, has already been successfully used in the procedures of low-temperature storage of ram semen (Fukui et al. 2008; Paz et al. 2010; Khalifa et al. 2013; Quan et al. 2015; Snoeck et al. 2017). The application of soybean lecithin is currently under the focus of research in sperm ultra-rapid freezing (Zakošek Pipan et al. 2020). All the above-mentioned make this readily available commercial semen extender attractive to try in the procedure of ram sperm ultra-rapid freezing, especially under farm conditions. Furthermore, and most importantly, in our study, the AndroMed semen extender was used for sperm ultra-rapid freezing of both, without and with 1,4-CHD extracellular ice inhibitor supplementation. Therefore, the comparison of the results obtained in the ultra-rapid freezing procedure on the intactness of spermatozoa ultra-rapidly frozen without, or with 1,4-CHD extracellular ice inhibitor must be fully valid, even so, the freezing medium used was not specially developed for ram sperm ultra-rapid freezing. Nevertheless, it could be assumed, that the usage of a freezing medium formulated optimally for ultra-rapid freezing could improve the overall results of the cryopreservation. Interestingly, our results on the preserved intact ram spermatozoa are in concordance with the results reported previously (Jiménez-Rabadán et al. 2015), where ultra-rapid freezing of ram sperm with egg yolk-free diluents (but modified by combinations of sucrose and glycerol) led to very low (around 1%) sperm viability, and only sperm vitrified with egg yolk-supplemented Biladyl extender showed some acceptable values of viability. The approach of using egg yolk-based (preferably, commercial) semen extenders as a freezing medium of choice could be an advantageous background for any further trial for the improvements in the ultra-rapid freezing procedure in ram, especially if it will be used together with any intracellular ice crystal growth inhibition approach.

Conclusions

In the present study, the approach of inhibition of the growth of extracellular ice crystals during cell freezing was chosen to test the cryodamaging role of intracellular ice in the model of ram sperm ultra-rapid freezing. According to the general aims of our study, we present the following obtained results: 1) the ability of 1,4-CHD to inhibit the growth of extracellular ice crystals in the freezing medium of choice (AndroMed) was confirmed physically with the use of X-ray diffraction analysis; 2) the nontoxic nature of 1,4-CHD upon chilled ram sperm cells was confirmed with the use of two flow cytometric panels; 3) the intactness of spermatozoa ultra-rapidly frozen without, or with 1,4-CHD extracellular ice inhibitor was compared flow cytometricaly. It was shown that the inhibition of extracellular ice by 1,4-CHD does not improve the results of ram sperm ultra-rapid freezing; 4) the destruction of the plasma membrane (possibly, induced by intracellular ice) on the ultra-rapidly frozen spermatozoa was observed in the presence of 1,4-CHD extracellular ice inhibitor with the use of scanning electron microscopy. Importantly, based on the obtained

results, we confirmed our hypothesis which is based on the simple mechanistic point of view: after the use of extracellular ice inhibitors and by so after the inhibition of the growth of extracellular ice crystals during cell freezing by ultra-rapid freezing, the cells should not lose their intracellular water fast enough, that should leads to spermatozoa cryodamage (mainly, on the level of their plasma membrane) due to formation of intracellular ice crystals. Therefore, we concluded that the intracellular ice plays the role in the sperm cryodamage, at least in the model of ram sperm ultra-rapid freezing. This should be considered in any further studies pointed to the search for an optimal strategy of how to improve low results of ram sperm ultra-rapid freezing procedure.

Disclosure statement

Funding

Availability of data and materials

All data generated or analyzed during this study are included in this published article.

ORCID

Martin Ptacek http://orcid.org/0000-0003-4438-3229
Ludek Stadnik http://orcid.org/0000-0002-7880-0089

References

Aires VA, Hinsch K-D, Mueller-Schloesser F, Bogner K, Mueller-Schloesser S, Hinsch E. 2003. In vitro and in vivo comparison of egg yolk-based and soybean lecithin-based extenders for cryopreservation of bovine semen. Theriogenology. 60(2):269–279. doi:10.1016/S0093-691X(02)01369-9.

Akçay E, Kulaksız R, Daskin A, Çebi Ç, Tekin K. 2012. The effect of different dilution rates on post-thaw quality of ram semen frozen in two different eggyolk free extenders. Slov Vet Res. 49:97–102.

Arando A, Delgado JV, Arrebola FA, León JM, Alcalá CJ, Pérez-Marín CC. 2019. Vitrification induces critical subcellular damages in ram spermatozoa. Cryobiology. 87:52–59. doi: 10.1016/j.cryobiol.2019.02.005. PubMed PMID: 30826334.

Arando A, Gonzalez A, Delgado JV, Arrebola FA, Perez-Marín CC. 2017. Storage temperature and sucrose concentrations affect ram sperm quality after vitrification. Anim Reprod Sci. 181:175–185. doi: 10.1016/j.anireprosci.2017.04.008. PubMed PMID: 28461086.

Barbas JP, Mascarenhas RD. 2009. Cryopreservation of domestic animal sperm cells. Cell Tissue Bank. 10(1):49–62. doi: 10.1007/s10561-008-9081-4. PubMed PMID: 18548333.

Bousseau S, Brillard JP, Marquant-Le Guienne B, Guérin B, Camus A, Lechat M. 1998. Comparison of bacteriological qualities of various egg yolk sources and the in vitro and in vivo fertilizing potential of bovine semen frozen in egg yolk or lecithin based diluents. Theriogenology. 50(5):699–706. doi:10.1016/S0093-691X(98)00175-7.

Bóveda P, Toledano-Díaz A, Castaño C, Esteso MC, López-Sebastián A, Rizos D, et al. 2020. Ultra-rapid cooling of ibex sperm by spheres method does

not induce a vitreous extracellular state and increases the membrane damages. PLoS One. 15(1):e0227946. doi: 10.1371/journal.pone.0227946. PubMed PMID: 31978160; PubMed Central PMCID: PMC6980613.

Daramola JO, Adekunle EO. 2016. Comparative effects of slow freezing and vitrification on cryosurvival of spermatozoa obtained from west African dwarf goat bucks. Cryo Lett. 37(2):123–128. PubMed PMID: 27224524.

David I, Kohnke P, Lagriffoul G, Praud O, Plouarboué F, Degond P, et al. 2015. Mass sperm motility is associated with fertility in sheep. Anim Reprod Sci. 161:75–81. doi: 10.1016/j.anireprosci.2015.08.006. PubMed PMID: 26364125.

Fukui Y, Kohno H, Togari T, Hiwasa M, Okabe K. 2008. Fertility after artificial insemination using a soybean-based semen extender in sheep. J Reprod Dev. 54(4):286–289. doi: 10.1262/jrd.20004. PubMed PMID: 18408351.

Fuller BJ. 2004. Cryoprotectants: the essential antifreezes to protect life in the frozen state. Cryo Lett. 25(6):375–388. PubMed PMID: 15660165.

Honaramooz A. 2012. Cryopreservation of testicular tissue. In: Katkov I, editor. Current frontiers in cryobiology: InTech. doi:10.5772/32338.

Isachenko V, Maettner R, Petrunkina AM, Sterzik K, Mallmann P, Rahimi G, et al. 2012. Vitrification of human ICSI/IVF spermatozoa without cryoprotectants: new capillary technology. J Androl. 33(3):462–468. doi:10.2164/jandrol.111.013789. PubMed PMID: 21719694.

Jiménez-Rabadán P, García-Álvarez O, Vidal A, Maroto-Morales A, Iniesta-Cuerda M, Ramón M, et al. 2015. Effects of vitrification on ram spermatozoa using free-egg yolk extenders. Cryobiology. 71(1):85–90. doi: 10.1016/j.cryobiol.2015.05.004. PubMed PMID: 26004240.

Khalifa T, Lymberopoulos A, Theodosiadou E. 2013. Association of soybean-based extenders with field fertility of stored ram (ovis aries) semen: a randomized double-blind parallel group design. Theriogenology. 79(3):517–527. doi: 10.1016/j.theriogenology.2012.11.009. PubMed PMID: 23219519.

Kratochvílová I, Golan M, Pomeisl K, Richter J, Sedláková S, Šebera J, et al. 2017. Theoretical and experimental study of the antifreeze protein AFP752, trehalose and dimethyl sulfoxide cryoprotection mechanism: correlation with cryopreserved cell viability. RSC Adv. 7(1):352–360. doi: 10.1039/C6RA25095E. PubMed PMID: 28936355; PubMed Central PMCID: PMC5602551.

Lv C, Wu G, Hong Q, Quan G. 2019. Spermatozoa cryopreservation: state of art and future in small ruminants. Biopreserv Biobank. 17(2):171–182. doi: 10.1089/bio.2018.0113. PubMed PMID: 30499684.

Miguel-Jimenez S, Rivera Del Alamo MM, Álvarez-Rodríguez M, Hidalgo CO, Peña AI, Muiño R, et al. 2020. In vitro assessment of egg yolk-, soya bean lecithin- and liposome-based extenders for cryopreservation of dairy bull semen. Anim Reprod Sci. 215:106315. doi: 10.1016/j.anireprosci.2020.106315. PubMed PMID: 32216928.

Morris GJ. 2006. Rapidly cooled human sperm: no evidence of intracellular ice formation. Hum Reprod. 21(8):2075–2083. doi: 10.1093/humrep/del116. PubMed PMID: 16613884.

Najafi A, Najafi MH, Zanganeh Z, Sharafi M, Martinez-Pastor F, Adeldust H. 2014. Cryopreservation of ram semen in extenders containing soybean lecithin as cryoprotectant and hyaluronic acid as antioxidant. Reprod Domest Anim. 49(6):934–940. doi: 10.1111/rda.12405. PubMed PMID: 25219460.

Paz P de, Esteso MC, Alvarez M, Mata M, Chamorro CA, Anel L. 2010. Development of extender based on soybean lecithin for its application in liquid ram semen. Theriogenology. 74(4):663–671. doi: 10.1016/j.theriogenology.2010.03.022. PubMed PMID: 20537695.

Ptáček M, Stádníková M, Savvulidi F, Stádník L. 2019. Ram semen cryopreservation using egg yolk or egg yolk-free extenders: preliminary results. Scientia Agriculturae Bohemica. 50(2):96–103. doi:10.2478/sab-2019-0014.

Quan GB, Li DJ, Ma Y, Zhu L, Lv CR, Hong QH. 2015. Cryopreservation of ram spermatozoa in the presence of cyclohexanhexol-derived synthetic ice blocker. Small Ruminant Res. 123(1):110–117. doi:10.1016/j.smallrumres.2014.11.007.

Quan GB, Wu SS, Lan ZG, Yang HY, Shao QY, Hong QH. 2013. The effects of 1,4-cyclohexanediol on frozen ram spermatozoa. Cryo Lett. 34(3):217–227. PubMed PMID: 23812311.

Rodriguez-Martinez H. 2012. Cryopreservation of porcine gametes, embryos and genital tissues: state of the art. In: Katkov I, editor. Current frontiers in cryobiology: InTech. doi: 10.5772/34429.

Savvulidi FG, Ptacek M, Malkova A, Beranek J, Stadnik L. 2021. Optimizing the conventional method of sperm freezing in liquid nitrogen vapour for Wallachian sheep conservation program. Czech J Anim Sci. 66(No. 2):55–64. doi:10.17221/226/2020-CJAS.

Shu Shan Z, Jian Hong H, Qing Wang L, Zhong Liang J, Xiao Ying Z. 2009. The cryoprotective effects of soybean lecithin on boar spermatozoa quality. Afr J Biotechnol. 8(22):6476–6480. doi:10.5897/AJB09.1070.

Snoeck PPN, Moura LCO, Silva MC, Machado-Neves M, Melo MIV, Heneine LGD, et al. 2017. Effect of storage conditions on the LDL effectiveness in ovine sperm cryopreservation. Cryobiology. 75:88–90. doi: 10.1016/j.cryobiol.2017.01.007. PubMed PMID: 28115174.

Tsuzuki Y, Kusao T, Ashizawa K, Fujihara N. 2000. Effect of different cryoprotectants on the survivability and the development of bovine oocytes matured In vitro. J Appl Anim Res. 18(1):15–24. doi:10.1080/09712119.2000.9706319.

Xin M, Niksirat H, Shaliutina-Kolešová A, Siddique M, Sterba J, Boryshpolets S, Linhart O. 2019. Molecular and subcellular cryoinjury of fish spermatozoa and approaches to improve cryopreservation. Rev Aquacult. 12 (2):909–924. doi:10.1111/raq.12355.

Zakošek Pipan M, Casal ML, Šterbenc N, Virant Klun I, Mrkun J. 2020. Vitrification using soy lecithin and sucrose: a new way to store the sperm for the preservation of canine reproductive function. Animals (Basel). 10(4). doi: 10.3390/ani10040653. PubMed PMID: 32283781; PubMed Central PMCID: PMC7222707.